

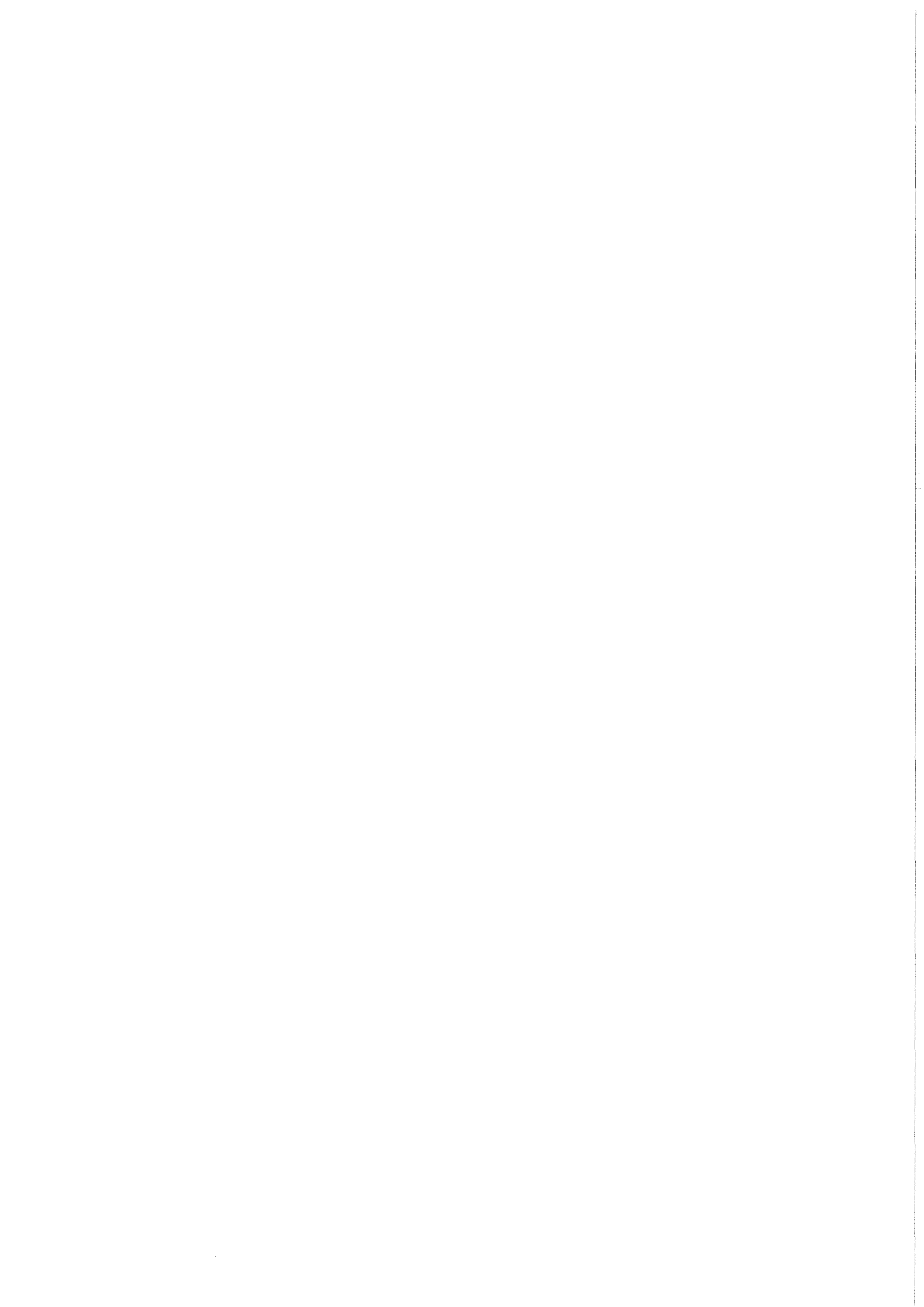
**KfK 3979
EUR 9611e
Oktober 1985**

Fusion Technology Programme

**Semi-annual Report
April 1985 - September 1985**

**Compiled by
D. Finken
Projekt Kernfusion**

Kernforschungszentrum Karlsruhe



KERNFORSCHUNGSZENTRUM KARLSRUHE

Projekt Kernfusion

KfK 3979

EUR 9611 e

Fusion Technology Programme

Semi-annual Report

April 1985 - September 1985

Compiled by

D. Finken

Kernforschungszentrum Karlsruhe GmbH, Karlsruhe

Als Manuskript vervielfältigt
Für diesen Bericht behalten wir uns alle Rechte vor

Kernforschungszentrum Karlsruhe GmbH
ISSN 0303-4003

CONTENTS

page

Preface		1
Description of Technical Work		
B 1	Blanket Design Studies	3
B 2	Development of Computational Tools for Neutronics	6
B 6	Corrosion of Structural Materials in Flowing $\text{Li}_{17}\text{Pb}_{83}$	7
B 9	Tritium Extraction based on the Use of Solid Getters	8
B 11 - B 16	Ceramic Breeder Materials	9
M 1	LCT-Project	13
M 3	Development of High Field Composite Superconductors	15
M 4	Superconducting Poloidal Field Coils	18
MAT 1	Post Irradiation Testing of Stainless Steel	20
MAT 6/MAT 13	Ceramics for First Wall Protection, Insulators and Windows	21
S+E 1	Radioactive Effluents: Behaviour of Gaseous Tritium in the Air, Plant, Soil System	23
S+E 2	Accident Analysis	24
T 1	Fuel Clean-up System	26
T 5	Development of Tritium Decontamination Systems	27
T 6	Industrial Development of Large Components for the NET Vacuum System	28
Studies for NET/INTOR		29
Development of ECRH Power Sources at 150 GHz		33
Publications		35
Appendix I:	Participation of KfK Departments in the Fusion Technology Programme	36
Appendix II:	Table of NET Contracts	37
Appendix III:	KfK Departments and Project Management Group	38

P r e f a c e

KFK is involved in the European Fusion Programme predominantly in the NET and Fusion Technology part. The following fields of activity are covered:

- Studies for NET, alternative confinement concepts, and needs and issues of integral testing.
- Research on structural materials.
- Development of superconducting magnets.
- Gyrotron development (part of the Physics Programme).
- Nuclear technology (breeding materials, blanket design, tritium technology, safety and environmental aspects of fusion, remote maintenance).

Reported here are status and results of work under contracts with the CEC within the NET and Technology Programme.

The aim of the major part of this R & D work is the support of NET, some areas (e.g. materials, safety and environmental impact, blanket design) have a wider scope and address problems of a demonstration reactor.

In the current working period, several new proposals have been elaborated to be implemented into the 85/89 Euratom Fusion Programme. New KfK contributions relate to materials research (dual beam and fast reactor irradiations, ferritic steels), to blanket engineering (MHD-effects) and to safety studies (e.g. magnet safety).

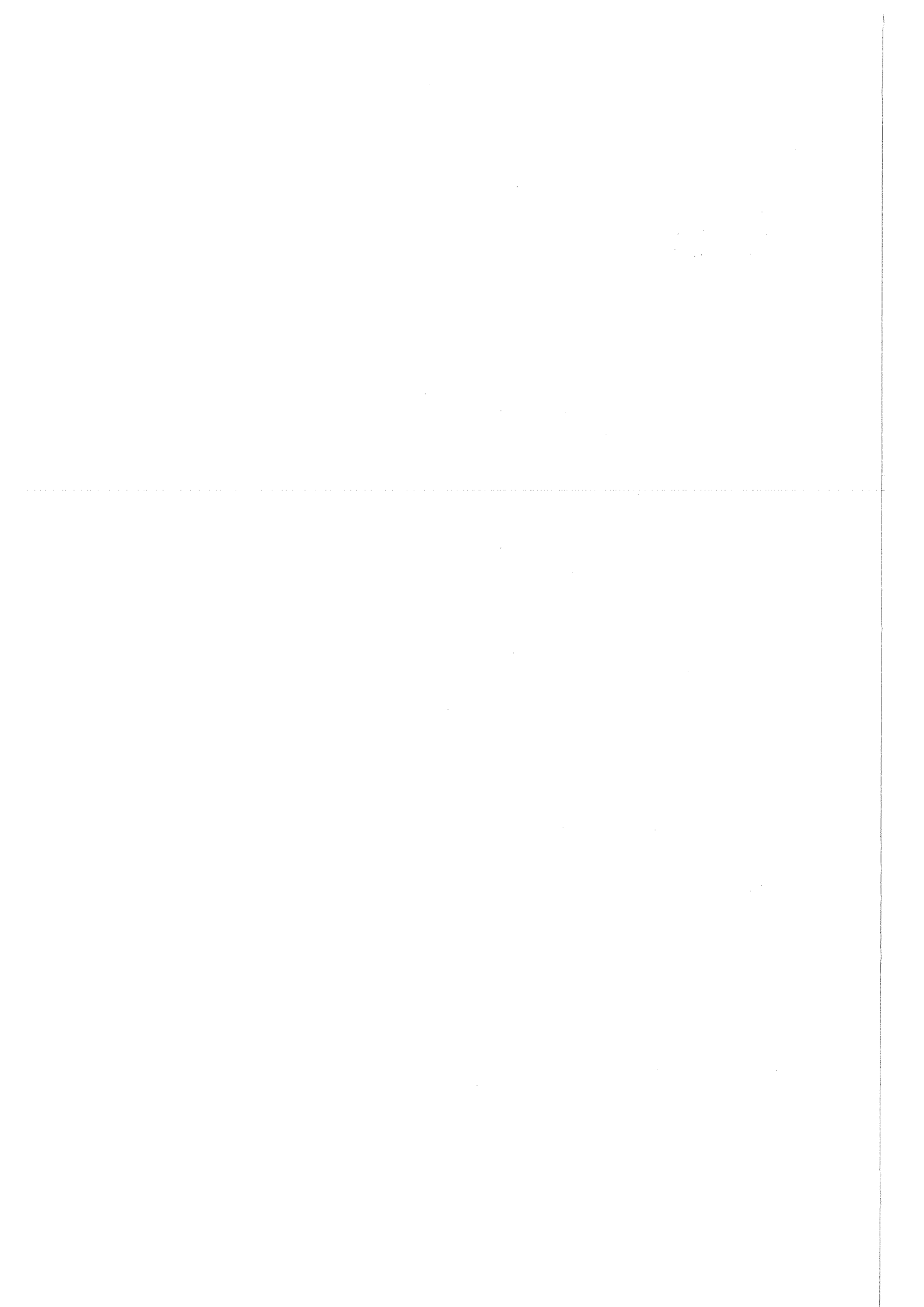
Significant progress has been made in most areas of the project. Notable achievements were:

- Commissioning of the dual beam facility.
- Start of detailed planning for the KfK Tritium Laboratory.
- Elaboration of a conductor concept for poloidal field coils.
- Installation of the LCT coil at ORNL completed.
- Placement of the first research contract on large vacuum components for NET to industry.

Detailed progress is subject of this report.

Cooperation with the NET-Team, the Joint Research Centres, the Associations and the US laboratories has grown and has essentially contributed to the progress of the work.

J.E. Vetter



B 1 Blanket Design Studies

Helium Cooled Ceramic Breeder Blanket

The design studies of a NET blanket with Li_4SiO_4 breeder and helium coolant were continued. In the last semi-annual report the difficulties encountered with a lobular blanket similar to the GA design were mentioned. Thus, this concept was abandoned and a new concept with self sustaining elements has been developed. It is illustrated in Fig. 1 and Fig. 2.

The blanket consists of toroidally arranged nearly rectangular canisters, filled with a bed of Li_4SiO_4 pebbles, surrounded by helium at 1 bar pressure. The coolant helium flows at 60 bars in tubes which pass through the bed as shown in Fig. 2. Each canister is segmented by steel stiffing plates. Manifolds for coolant supply are arranged on the back side of the canisters. At the front part, within the canister but separated from the breeder, a 1000 mm thick beryllium layer is located, which is cooled by the same tubes as the breeder.

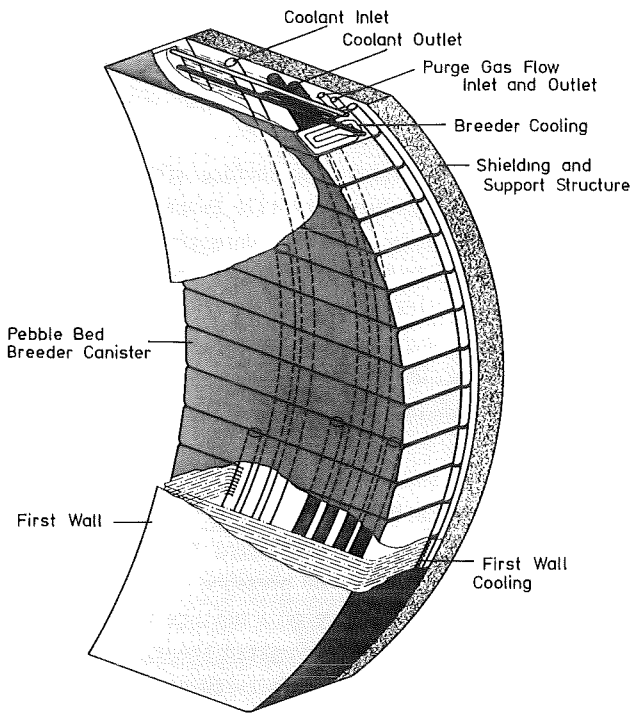


Fig. 1: Helium cooled ceramic breeder blanket segment

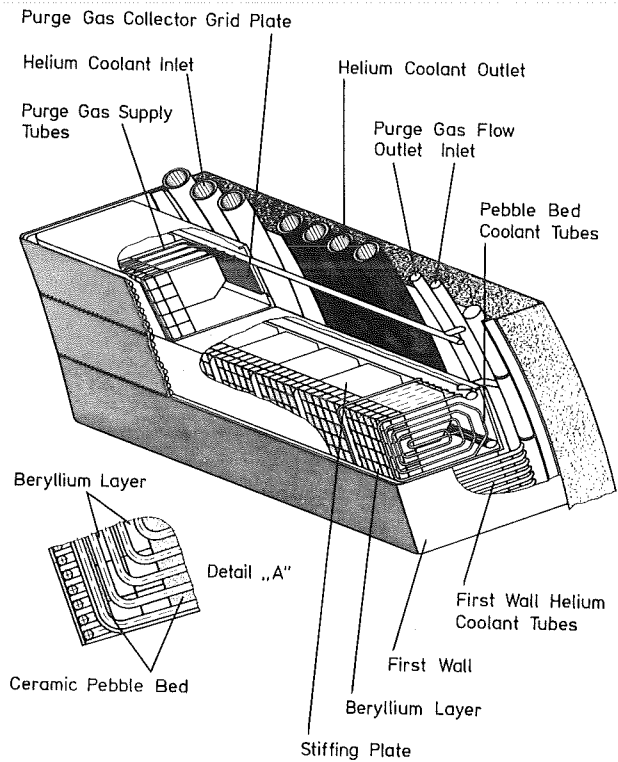


Fig. 2: Detail of the canister of the helium cooled ceramic breeder blanket.

Purge gas is fed through perforated tubes near the first wall and flows radially through the blanket to a collector grid plate. The tritium breeding rate is enhanced by nearly 20% when a 1 cm layer of breeder material is located between beryllium and first wall. A design to accommodate this layer is in development.

The breeder canisters are enclosed in a helium cooled first wall cooled by helium tubes running in radial-toroidal-radial direction. The helium coolant flows in series first through the breeder region. By the assembly of the blanket segments all canisters are first mounted, then the first wall sections are welded to each other, so that each blanket segment is totally encapsulated by a first wall container.

Care was taken in the design to accommodate for the differential thermal expansion effects. The canisters are fixed to the coolant outlet tubes and follow their thermal expansion. By a sliding attachment forces are transferred to the support structure from a second rigid part. With the support structure kept at 200°C the thermal stresses can be accommodated. The two structures are connected by the thin and relatively flexible first wall coolant tubes

It is important that the bed of pebbles is flowing with low inner friction to avoid damage of the pebbles and deformation of the canister walls during thermal cycling. Experiments are planned to investigate the behaviour of ceramic pebble beds under temperature variations as well as the heat transfer inside the bed.

Liquid Metal Cooled Blanket

The investigation of different methods for tritium extraction from $\text{Li}_{17}\text{Pb}_{83}$ with the emphasis on the conditions of a selfcooled blanket has continued (see also B 9). Use of a secondary liquid metal such as sodium (Na) or sodium-potassium, (NaK) which is processed in cold traps for tritium extraction, has been found promising. The tritium is permeating either through the walls of the intermediate heat exchanger or through a separate permeation window made of vanadium, resulting in partial tritium pressure in the lithium lead of 10 Pa or 1 Pa, respectively. Cold trapping of Na at 115°C leads to tritium partial

pressure in the secondary liquid metal of 10^{-2} Pa. The use of NaK with a cold trap temperature of 30°C would lower this pressure by a factor up to 100.

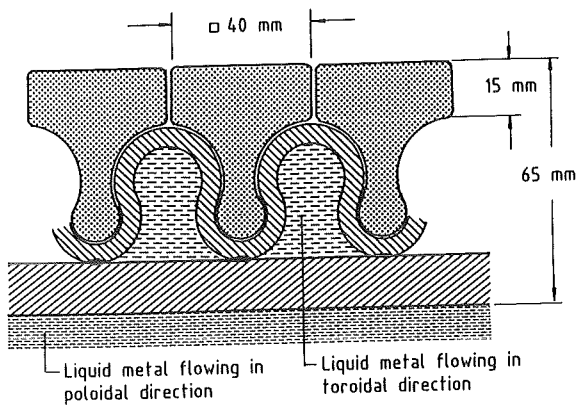
Two design concepts have been envisaged for the use of a secondary liquid metal loop. One solution is based on the use of secondary loops of nearly identical capacity as those used in the SNR-300 fast breeder reactor. A probably more simple solution is a double wall heat exchanger with Na or NaK flowing through the gap between the two walls. Tritium permeation losses are small enough for both concepts in order to avoid the reprocessing of the cooling water in isotopic separation plants.

The protection of the first wall by ceramic materials has been investigated. This design study is restricted to radiatively cooled tiles in order to limit the scope and the range of parameters. There are basically three requirements for a suitable method of mechanical tile attachment:

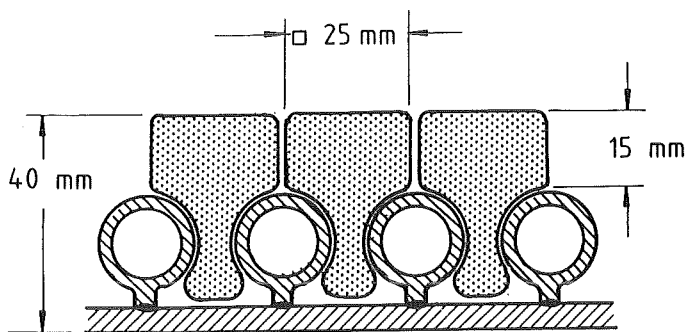
- a) A large ratio of radiating surface with respect to front surface reduces the tile temperature.
- b) Small tile dimensions and unrestricted thermal expansion result in lower thermal stresses.
- c) Short heat flow paths lead to lower maximum temperatures and thermal stresses.

Design concepts which take these requirements into account are shown in Figures 3a and 3b.

The first wall, shown in Fig.3a, is an integral part of a selfcooled blanket with liquid metal flowing in toroidal direction in order to cool the first wall without excessively large MHD pressure drop. The tiles of graphite, silicon carbide or a mixture of both are fitted loosely into the corrugated sheet. The heat transferring surface is more than twice as large as the plasma facing surface, leading to tile temperatures as low as possible achievable by radiation cooling and to relatively small temperature differences in the toroidal cooling channels. The design allows for unrestricted thermal expansion of the tiles and results together with the small dimensions in minimal thermal stresses. An additional advantage is the possibility to exchange eroded or broken tiles without blanket exchange.



a) Integral first wall for a liquid metal cooled blanket



b) Separate first wall (gas cooled)

Fig. 3: Radiatively cooled protection tiles

A similar attachment of protection tiles has been investigated for a separate first wall concept. In this case, gas cooling is provided which makes the design of the first wall box suitable for gas cooled, water cooled and liquid metal cooled blankets. A vertical cross section of such a first wall is shown in Fig. 3b.

Experiments with liquid metal to support liquid metal fusion blanket designs are planned to investigate Magneto-Hydro-Dynamic (MHD) pressure drop in straight

ducts, sharp bends and in a "poloidal-toroidal" test section. A normal conducting Bitter magnet of 6.5 tesla field strength and superconducting dipole and solenoid magnets with 4.5 and 3.5 tesla field strength, respectively, are used to create the magnetic field volume for the tests.

A movable sodium-potassium loop with a flow rate of $25 \text{ m}^3/\text{h}$ and a pressure head of 25 bars which will be used for the above mentioned experiments is under construction. Development of techniques to measure local velocities in liquid metal under MHD conditions has been started.

Theoretical work is under way where simple working models and improved scaling laws shall be derived and based on these models more sophisticated design codes shall be developed.

Staff:

- L. Barleon
- E. Bojarsky
- M. Dalle Donne
- S. Dorner
- U. Fischer
- H. Kreuzinger
- M. Küchle
- S. Malang
- I. Michael
- H. Reiser

B 2 Development of Computational Tools for Neutronics

For a rigorous treatment of the anisotropic scattering of neutrons in fusion reactor blankets, a general transport system, GANTRAS, is under development at KfK. The one-dimensional module ANTRA1, which is based on the ONETRAN-programme, has been set up for spherical and plane geometries. At present, ANTRA1 is extended to include also the cylindrical geometry option. This is an essential link to the two-dimensional module.

Numerical tests with ANTRA 1 have been performed for a Be-sphere surrounding a 14 MeV (inhomogeneous source calculations), and for a critical uranium assembly, to check the k_{eff} -calculation. The results were compared to the S_N - P_3 -calculation performed with ONETRAN (see Table 1), using the same data base.

To process double-differential cross-sections (DDX), needed for the GANTRAS-system, a new system of processing codes had to be assessed. For handling and processing the DDX-data for continuous neutron scattering, which will be contained on the forthcoming European Fusion File EFF, the ECN/Petten-code GROUPXS was implemented. Since GROUPXS uses the Legendre-representation for the DDX-data as well as for the scattering matrices, the code was extended to be able to calculate group-averaged, angle-segmented DDX-data (i.e. full 3-d scattering matrices) by starting from an angle-pointwise data file. Next it is intended to introduce a new scheme for the transformation from the center-of-mass to the laboratory system by avoiding the Legendre-representation for the DDX-data in the laboratory system. This procedure will be appropriate for a rigorous treatment of the anisotropic neutron scattering. Finally the modules for processing the DDX-data for elastic and discrete inelastic neutron scattering (by using single-differential angular distributions) will be developed.

The NJOY processing code has been implemented at KfK to calculate group constants in ENDF/B-format for conventional cross-section types. A comparison between

group constants calculated by NJOY and by the KfK processing code MIGROS has been performed for the heavy nuclides U^{235} and Pu^{238} . An overall satisfactory performance was found. This comparison study will be continued in more detail. At present, an auxiliary module is written, which creates an appropriate interface between NJOY and the KfK-processing-codes.

At KfK two Monte Carlo codes, MCNP-3 and TRIPOLI-02, have been implemented. A thorough comparison study referring to the calculational procedure, the data base, the code handling, the input preparation, etc. of the two codes is being performed.

The VITAMIN-C library has been transformed to the KAPROS programme system. This enables us to use VITAMIN-C together with KfK data and processing codes and thus to modify and/or improve the VITAMIN-C library in a convenient way.

	ONETRAN		ANTRA1 *	
	isotropic (P ₀)	anisotropic (P ₃)	isotropic (DDX)	anisotropic (DDX)
M	1.546	1.490	1.546	1.510
L	1.498	1.447	1.498	1.468

Table 1: Multiplication (M) and Leakage (L) for a Be-sphere of 5 cm thickness (with a 14 MeV neutron source in the centre), calculated by ONETRAN and ANTRA1

* The anisotropic scattering matrices used in these test calculations were created from the same P_0 - and P_3 -scattering matrices, respectively, from VITAMIN-C as those used in the ONETRAN calculations.

Staff:

C. Broeders
 I. Broeders
U. Fischer
 B. Goel
 B. Krieg
 H. Küsters
 A. Schwenk
 E. Stein
 E. Wiegner

B 6 Corrosion of Structural Materials in
Flowing Li₁₇Pb₈₃

Staff:
Ch. Adelhelm
H.U. Borgstedt
G. Drechsler
G. Frees
M. Grundmann
Z. Peric

The first corrosion test in the pumped LiPb loop was terminated after 500 h duration. Tube specimens of AISI 304 steel, diameter 8 mm, wall thickness 1 mm, length 70 mm, were exposed to the liquid eutectic at a temperature of 400-420°C depending on the position in the test section. The molten metal completely wetted the specimens.

After the exposure, the specimens were taken out of the loop. The specimen holder was difficult to dismount due to the brazing action of the eutectic. Most of the adherent lead was removed by means of a washing procedure in molten sodium. Some lead, however remained on the surfaces and could only be removed by means of a treatment with a mixture of acetic acid and hydrogen peroxide.

In spite of this absorption of lead, the most of specimens lost weight. The highest weight losses indicated effects similar to values published by the ANL /1/. SEM examination of the corroded surfaces demonstrated that lead was concentrated on the spots of the surfaces, which had suffered the strongest corrosion effects. The lead most probably penetrated the steel specimens at several locations, while other parts of the surface remained more or less unaffected. The maximum corrosion rate estimated from weight loss data was $R = 45 \mu\text{m/a}$ at the temperature of 420°C. Further examinations are underway, a second corrosion test with the same material is running.

Analytical studies of the LiPb eutectic showed that the losses of Li were only small. The contents of iron, chromium and even nickel after the corrosion test were below the detection limit. First oxygen estimations indicated oxygen contents in the 10^{-3} level, though the results were scattering.

/1/ O. Chopra, D.L. Smith, J. Nucl. Mat. 122 & 123 (1984) 1219-1224

B 9 Tritium Extraction based on the Use of Solid Getters

Several methods were proposed to extract tritium from the $Li_{17}Pb_{83}$ breeding material. Task B9 will study the use of solid getters in direct contact with the liquid metal.

The experiments to study the uptake of hydrogen from the gas phase by different getter materials continued for lower partial pressures. The investigated pressure range of 0.01 to 2 mbar is usually not reported in the literature.

The following materials have been proved to be suitable to extract hydrogen from the gas phase at low pressures.

getter metals as received	temperature range °C
V, Y as foils Nb as granules Ti, Zr as sponge	400 to 500
Ti, Zr, Nb as foils La as granules	500 to 600
Ta as foil	> 600

In these cases, the initial pressure dropped from 10^{-1} to 10^{-3} mbar within one hour.

Because of the small mass transfer coefficients at low pressures, the temperatures are higher compared to the experiments at higher pressures.

The temperature influences as well as the hydrogen solubility and the equilibrium-pressure.

With V-foil at 400 °C the pressure is reduced from 1.5×10^{-2} to 4.5×10^{-3} mbar within 30 minutes. For this equilibrium pressure 80 appm hydrogen were dissolved in the metal, and the Sieverts constant K_s was 1.2×10^3 (appm/mbar^{1/2}). A similar experiment was performed with Nb-foil at 550 °C. The pressure dropped from 10^{-1} to 3×10^{-2} mbar within 60 minutes, the concentration in the metal was 300 appm H, the Sieverts constant 1.6×10^3 . The values for K_s are about one magnitude lower if compared to values from the literature obtained for higher pressures /1/.

Another example will be given for lanthanum. Having a loading of 0.06 hydrogen atoms per La-atom, the following hydrogen partial pressures were found:

500 °C	2.0×10^{-4} mbar
550 °C	1.5×10^{-3} mbar
600 °C	7.0×10^{-3} mbar

A very important point of the investigations will be the study of the compatibility of the getter materials with the liquid metal. An apparatus is ready now for such tests in vacuum or inert gas and in the temperature range of 300 to 800 °C. Experiments can be done with static or stirred $Li_{17}Pb_{83}$. Besides getter materials also some other materials will be studied, which may be used as coatings for getter metals, e.g. Ta, Mo, Hf, W and others.

During the text reporting period especially compatibility studies will be done. Also hydrogen dissolution in getter materials, submerged in liquid $Li_{17}Pb_{83}$, will be investigated.

/1/ E. Veleckis, J.Phys.Chem. 73 (1969) 683

Staff:

H. Feuerstein

G. Gräbner

B 11-16 Ceramic Breeder Materials

1. Fabrication and Characterization of Ceramic Breeder Materials (B11/12)

The preparation and fabrication of lithium containing monosilicates are under development to be used as breeder materials for fusion reactors within the European fusion programme (Tasks B11-B12). The high lithium containing compounds, such as Li_4SiO_4 and the up to now not established compounds Li_6SiO_5 and Li_8SiO_6 are of special interest within this programme. Based on the experience gained in the fabrication of Li_2SiO_3 and Li_4SiO_4 a similar method has been worked out for the preparation of a compound with the stoichiometric composition of Li_6SiO_5 and for the preparation of Li_4SiO_4 specimen, which can be sintered to high density.

A number of Li_2SiO_3 and Li_4SiO_4 pellets were prepared to obtain information on the physico-chemical and mechanical properties as well as on the irradiation behaviour, based on the preparation method already described in detail. The samples were especially prepared for irradiation tests in Grenoble (SILOE-reactor) and Saclay (OSIRIS-reactor); for an exchange of samples between the French and German groups to compare the methods of characterization, and for a compatibility test with beryllium metal.

A preparation method for a compound with the stoichiometric composition of Li_6SiO_5 has been worked out. This compound was prepared from alcoholic suspensions of stoichiometric amounts of lithium hydroxide, LiOH , and amorphous silica, SiO_2 (Aerosil), in ethanol or in isopropanol. Powders with a Li/Si-ratio of 6:1 were obtained from those suspensions after distillation of the alcohol and drying of the powders at about 110°C . Sintered specimens of the powders were obtained after calcination at 400 to 500°C , pressing into pellets, and sintering at temperatures of up to 700°C .

It was found from x-ray and scanning electron microscope studies, that a crystalline material had formed with a six-edged plate like crystal habitus. The x-ray diagram showed reflection lines which were

different from the known lithium silicates. The chemical analysis of the Li/Si-ratio led to values of $\text{Li}:\text{Si} = 6:1$. Samples which were annealed at temperatures higher than 700°C , showed the formation of lithium orthosilicate, Li_4SiO_4 , and lithium oxide, Li_2O , which under the given experimental conditions evaporated. This was confirmed by chemical analysis where a Li/Si-ratio of 4:1 was found. From this, it is obvious that this compound decomposes at temperatures above 700°C . We assume the formation of a Li_6SiO_5 compound prepared by this method, even if it is not yet completely confirmed. In a similar way, formation of Li_8SiO_6 can likely be prepared.

The preparation of Li_4SiO_4 powders of stoichiometric composition from alcoholic suspensions by the same technique as above leads after calcination to Li_4SiO_4 powders which can be sintered at temperatures of up to 1100°C to densities of higher than 90 % th.d.

2. Measurement of physical, mechanical and chemical properties of ceramic breeder materials (B13)

Chemical Analysis

Lithium silicate powders and pellets of different stoichiometry from KfK fabrication have been chemically analysed determining the main components and impurities. For silicon and lithium analysis, samples have been decomposed by fusion with borates, disintegration in acid and AAS-analysis.

The same solution can be used for impurity-analysis, but the detection limit with AAS of some metallic elements can be reduced by separating the interfering silicate matrix with hydrofluoric acid.

Lithium silicates fabricated by spray-drying absorb CO_2 and H_2O . Their content was determined by two different analytical procedures. CO_2 was measured by coulometric titration after it had been extracted from the powder by means of phosphoric acid and transported by an inert carrier gas into the coulometric cell. In a separate step H_2O was released, together with CO_2 , at 900°C and selectively determined by coulometric Karl Fischer titration.

Constitution and Thermodynamics

The relative linear thermal expansion of lithium metasilicate, Li_2SiO_3 , has been measured by X-ray diffraction at temperatures between 300 and 1000°C in air. The curve is shown in fig. 4, it is in relatively good agreement with earlier results of dilatometer measurements up to 500°C (B. Schulz, KfK, private communication).

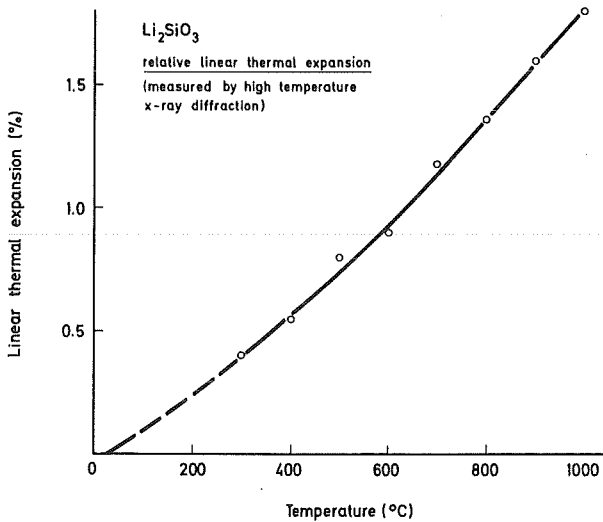


Fig. 4: Relative linear thermal expansion, measured by X-ray diffraction.

High temperature X-ray diffraction was used to study the reaction behaviour of spray-dried powders during the calcination step of the Li_4SiO_4 preparation via alcoholic suspensions.

The experiments for the study of the absorption of water vapor by Li_2O and Li_4SiO_4 were continued. Up to now, no indications were found for the formation of hydrated phases or hydroxides in the system $\text{Li}_4\text{SiO}_4\text{-H}_2\text{O}$. The measurements of H_2O partial pressures $\lesssim 250$ vpm are not yet reproducible. A thermal microbalance has been set in operation, first pretests are running at present.

Physical and mechanical properties

Numerical data of thermophysical, thermochemical, and also some mechanical properties of ceramic breeder materials were compiled. The main importance was given to special heat, thermal conductivity, linear thermal expansion, density, and melting point.

For the determination of Young's modulus and of the compressive strength of Li_2SiO_3 samples, pellets of various laboratory manufacturing series with different densities and microstructures were available. All manufacturing series have been characterized by ceramographic methods. Depending on the fabrication parameters there are considerable differences in the grain sizes and in the pore structures. The Young's modulus were evaluated from the ultrasonic velocity which was determined by the pulse-echo method. For the determination of the compressive strength the load was applied at a rate of 100 N/s (pellet diameter 8.5mm). The results obtained up to now are shown in Table 2. The diameters of the pellets are generally between 8.5 and 10.3 mm and the heights between 8.5 and 10.5 mm.

The measuring series of the creep rate under uniaxial compressive load in the temperature range between 800 and 900°C have been continued. A second experimental device has been installed.

Series	Density % TD	E GPa	σ MPa
III	70 - 83	35	100
IV	92	55	250
V	78	10	110
VI	83	30	255
VII	85	40	300
VIII	93	60	360

Table 2: Young's modulus E and compressive strength

3. Compatibility with stainless steels

The annealing tests with Li_2O , Li_2SiO_3 , and Li_4SiO_4 powder samples pressed into cladding material capsules were continued. The cladding materials were SS 316 and, recently, a martensitic-ferritic stainless steel (about 11% Cr, 0.5% Mo, German material number 1.4914). The reactive oxygen surplus was alternatively given by controlled H_2O or NiO additions. Annealing tests were conducted at 600, 700, and 800°C for 125 and 500 h. A first survey of the results suggests that there was no major difference in the cladding attack produced with H_2O or NiO. Concerning the cladding material, 1.4914 seemed to be no worse than 316, as far as the fine-grained martensitic microstructure was preserved.

4. Irradiation Testing of Ceramic Breeder Materials

A first irradiation of 45 German Li_2SiO_3 sample columns (about 360 pellets) DELICE 01 has been finished in the OSIRIS reactor at Saclay by end of January 1985. The transport of the irradiated samples to the KfK hot cells has been delayed by more than half a year because of licencing problems in France, it is now foreseen for end of September 1985. To investigate the tritium release and to remove the tritium from the sample for other post-irradiation examinations, installations were tested in glove boxes located in the hot cells to handle the irradiated stainless steel capsules containing the samples. The second B15 experiment DELICE 02 in the OSIRIS reactor is specified for 20 lithium meta- and lithium orthosilicate sample columns. Irradiation is planned for January 1986.

5. Tritium Recovery from Ceramic Breeder Materials

LILA1, the first CEA test of an experimental train for continuous measurement of tritium release from four lithium aluminate samples under irradiation, has been performed in the SILOE reactor at Grenoble. Based on the results of LILA1, some modifications of the experimental device have been made for the first KfK irradiation (LISA 1): Additional purification stages for water vapor at the purge gas inlet, capsules made

of stainless steel instead of quartz, reduction of oxidized tritium by a Zn bed, addition of 0.1 % H_2 to the He purge gas. Five KfK lithium silicate sample columns (Li_2SiO_3 and Li_4SiO_4) and one CEA lithium aluminate stack for comparison with LILA 1 results will be irradiated in LISA 1. The KfK samples have been sent to Grenoble and the irradiation is expected to start mid of September 1985.

6. The solubility of hydrogen in solid breeding materials

One of the objectives of NET is to demonstrate the feasibility of tritium breeding in a tokamak reactor. In this context relevant data on the behaviour of hydrogen in candidate breeding materials are needed for evaluation purposes.

In the past, numerous investigations have dealt with the determination of diffusion coefficient for tritium in ceramic breeders such as Li_2O , LiAlO_2 , Li_2SiO_3 , etc. Though equally important for an assessment of candidate lithium compounds, the tritium solubility in these solids has remained largely ignored. To fill this gap a programme has recently been started at KfK.

So far approx. 1200 pellets of Li_2Si_3 , having a diameter of 5.7 mm and a height of 1 mm, as well as several hundred pellets of Li_2SiO_3 and Li_4SiO_4 having a diameter of 4.5 mm and a height of 9 mm have been pressed from granular powder employing conventional techniques. Powders were either of commercial origin or synthesized at KfK by an improved spray dry method /V19929, 21158/. Lithium silicates are known to be aggressive chemicals. To reduce incorporation of the metal into the pellets during pressing a carefully cleaned and waxed (stearic acid) die in a dry atmosphere was employed for compaction. Sintering was carried out in an oven programmed up to 1100°C. Promising results were also obtained by hot impact densification. So far, the samples have been characterized by thermogravimetry, differential thermal analysis, heat Guinier, etc. With the latter technique the reversible and probably displacive transformation of orthosilicate that occurs at 680°C became clearly apparent.

The results also suggest that heating of Li_4SiO_4 up to high temperatures causes the formation of some Li_2SiO_3 .

measured, will be followed with a capacitive differential transducer in the temperature range 400 - 600°C. In addition experiments with H_2/D_2 as well as with tritium have been planned. Nearly 500 Ci of tritium are available as uranium tritide in a double walled container designed for circulation of the gas. The partial pressure of tritium can be determined with a small ionization chamber (3 ml volume) that has been constructed and successfully tested with tritium.

In complementary experiments, the solubility of hydrogen in Li_2SiO_3 has been examined in a 10 ml autoclave at a constant pressure of 70 bar and temperatures of 400 and 500°C, as a function of time. Results of still preliminary character suggest a solubility of the order of atom fraction $\geq 10^{-3}$.

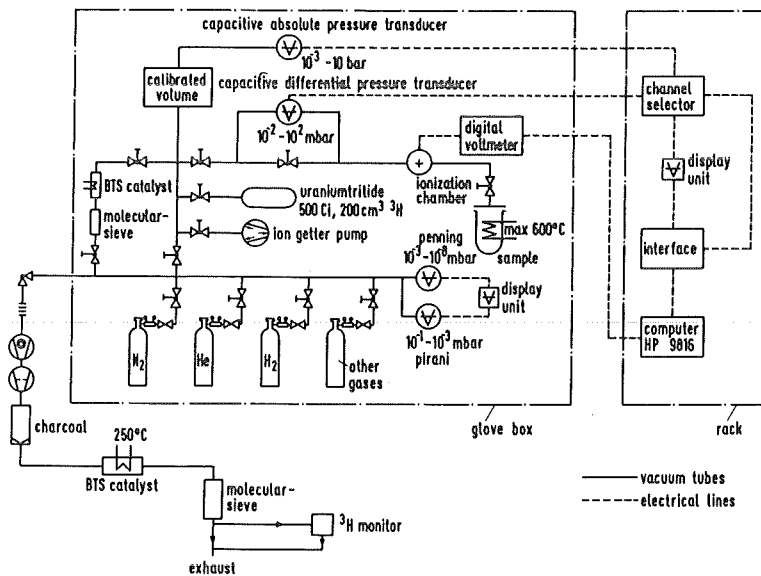


Fig. 5: Scheme of the apparatus for solubility measurements

During the last few months an apparatus, shown schematically in Fig. 5, has been build. The UVA equipment is designed for a volumetric hydrogen solubility measurement. Pellets will first be dried in an appropriate containment under high vacuum at elevated temperatures ($\sim 900^\circ$). After that, the closed containment will be transferred into a glove box having a very dry atmosphere ($< 1 \text{ ppm } \text{H}_2\text{O}$) and opened. The pellets will then be stacked inside a 70 ml aluminium vessel coated from the inside with a $1 \mu\text{m}$ thick Al_2O_3 film to minimize hydrogen permeation. The sample vessel will then be transferred into the inert gas glove box containing the UHV equipment and attached to the apparatus. Pressure increase or decrease, depending on whether hydrogen uptake or release is

Staff:

- Ch. Adelheim
- M. Blumhofer
- E. Bojarsky
- W. Breitung
- W. Dienst
- B. Dörzapf
- H. Elbel
- M. Glugla
- Ch. Gosgnach
- E. Günther
- H.E. Häfner
- R. Hanselmann
- J. Heger
- P. Hofmann
- W. Jahraus
- E. Kaiser
- D. Kempf
- K.-H. Kurz
- W. Laub
- H. Nagel
- R. Penzhorn
- V. Schauer
- R. Scherwinsky
- G. Schlickeiser
- K.H. Simon
- A. Skokan
- H. Strömann
- D. Vollath

Publications:

- 21158
- V 19929

- H. Wedemeyer
- H. Werle
- M. Wittmann
- H. Zimmermann

M 1 LCT-Project

The installation work is now complete for four coils (JAERI, General Dynamic/Convair, Swiss, Euratom) and in running for two coils (General Electric, Westinghouse), (Fig. 6).

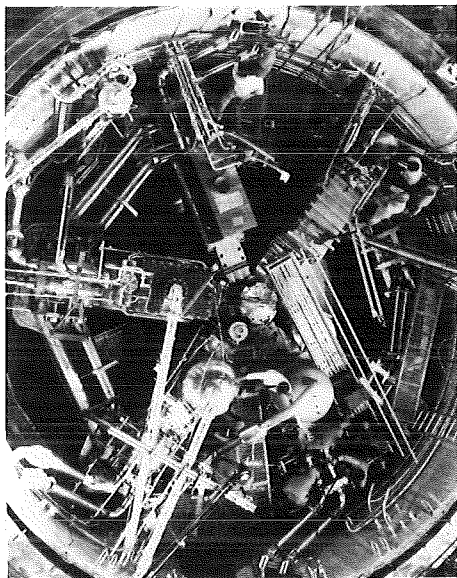


Fig. 6: The top view of the LCTF vacuum vessel with five installed LCT coils on May, 1985. (From left to right: EURATOM-, SWISS (BBC)-JAERI-, General Dynamic/Convair and General Electric Coil). Between EURATOM and General Electric Coil, the Torque beam with the pulse coil is visible.

Tightness problems with current feedthrough insulators of the Westinghouse coil led to a slip of the delivery date and necessitated a change of the feedthroughs. The change requires an insulation break in the superconducting bus. Euratom/KfK was asked to fabricate and to test fiber glass reinforced epoxy insulation breaks, because such breaks were successfully used in the Euratom LCT coil. No other solution was found which fitted in the present time schedule. Two breaks were fabricated, tested and sent to Oak Ridge in time.

In the reporting period the superconducting bus together with the vapour cooled leads for the Euratom LCT coil were installed, leak checked and high voltage

tested. All capillary tubes for mass flow measurements were carefully leak checked and one capillary tube with a flaw had to be replaced. The differential pressure transducers belonging to mass flow measurements were taken into operation, instrumentation and data acquisition were coupled to the experiment.

Euratom/KfK participated with one expert in the refrigerator test in April 85. Weak points (pressure drop across the purifier, operation temperature for forced flow cooled coils) were identified. The evaluation of the test is running.

The present goal to have all six coils and the pulse coil system installed to close the lid of the LCTF vacuum vessel at October 25, 1985 is on schedule.

The U.S. Department of Energy plans to terminate the LCT Project by September 87. In order to meet this boundary conditions the Operating Agent proposed a "Baseline Test Programme" for the test of the six coils. This Programme was derived from an existing test programme with minor changes.

This US proposal is subject to discussions of a subcommittee meeting of the FPCC, scheduled for September 16, 1985.

The TESPE Experiment

The six coil tests at normal operation conditions (including fast discharge) were performed successfully from both the cryogenic and the electrical point of view. Smooth cooldown to stable operation was achieved within 175 hrs. The maximum temperature difference within the total mass to be cooled could be kept below 50 K. Cryogenic operation at LHe temperature was automatically controlled and proved to be stable.

The design values of 7 kA, 7T and 8.8 MJ were reached at the first attempt without a "natural" quench. The maximum current chosen was 7.18 kA, corresponding to 85% of the short sample value, taken along the load line. Stresses of the coil casing were found to vary from 26 up to 49 MN/m², close to data calculated with a finite element program. Operation of quench

detection and energy dump circuits were tested by local heating of the conductor producing a normal zone. After quench detection the stored energy was dumped in an external resistor of 0.123Ω . The time needed from the heat pulse to completion of current transfer was 0.1 s. With a dump voltage of 840 V and a time constant of 2.3 s, 90% of the stored energy were dissipated outside the cryostat. The other 10% were lost in windings and casing. Eddy currents heated the casing to about 10 K (Fig. 7) and caused normal zones in the windings, the temperature of which reached up to 33 K by ohmic heating in the normal zones.

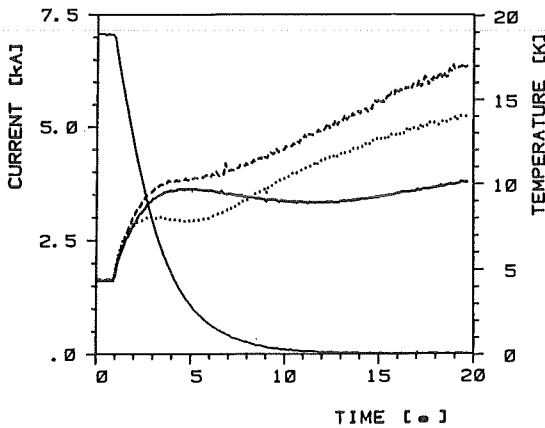


Fig. 7: Temperature rise in the coil casing due to eddy currents during fast safety discharge of stored energy.

The pressure within the helium space increased to roughly 0.5 MPa. After a dump, stable cryogenic operation was achieved again typically within one hour. The behaviour did not change significantly when no heat pulse preceded the energy dump.

The torus has shown its functionability for normal operation and it is now being prepared for experiments with respect to magnet safety. In order to study the magnetomechanical behaviour two buckling experiments

were performed. An effect of mechanical self-strengthening of the torus under operation was found. The measured data are being evaluated.

Staff:

- H. Bayer
- P. Duelli
- S. Förster
- G. Friesinger
- W. Geiger
- A. Grünhagen
- W. Herz
- L. Hütten
- K.P. Jüngst
- H. Katheder
- H. Kiesel
- P. Komarek
- T. Krüger
- G.W. Leppelmeier
- J. Lühning
- G. Nöther
- G. Obermaier
- L. Schappals
- H. Schnauder
- F. Spath
- E. Süß
- M. Süßer
- A. Ulbricht
- H. Veit
- R. Wagner
- F. Wüchner
- G. Zahn

M 3 Development of High Field Composite
Superconductors

High field superconductors for the HOMER test facility

- a. Extension of the experimental possibilities in the HOMER test facility to tests at 1.8 K.

Cooling of NbTi superconductors to 1.8 K allows for the maximum fieldstrength to be increased to about 12 T. Compared to Nb₃Sn (which can be used beyond that value), the better mechanical properties of the NbTi conductor can be advantageous.

The investigate conductors at current loads of up to 3 kA in a field of 12 T at superfluid He temperatures, the HOMER test facility was complemented by an 1.8 K insert. This modification was eased, because main components as the background magnetic field, power supply and current leads were already existing. In collaboration with a group of the CEN Saclay a custom taylored anticryostat was designed and built. The essential idea in the design of the 1.8 K cryogenic system was , to obtain fast and uncomplicated experimental operation avoiding a pollution of the 1.8 K refrigerator circuit with atmospheric nitrogen or oxygen during the change of a sample.

Therefore the LHe supply of the 1.8 K refrigerator and the LHe-bath of the experimental area are separated from each other. The LHe-bath is cooled down to 1.8 K by a heat exchanger.

The construction of the whole 1.8 K anticryostat system is finished. At present the system is being assembled in the HOMER facility and prepared for the first test.

- b. Heat treatment of 1000 m Nb₃Sn flat cable for a 15 T insert coil.

In the development work of a cryogenically stabilized Nb₃Sn conductor for a 15 T insert coil the conductor configuration was designed and tested by KfK. The manufacturing of the 1000 m long superconducting cable was shared between industry and KfK in the following way:

The industry is responsible for the components of the conductor (Nb₃Sn flat cable, the copper coated aluminum tape), and the soldering of these components. The heat treatment of the Nb₃Sn flat cable, a very delicate step of manufacture due to the brittleness of the conductor, will be done by KfK.

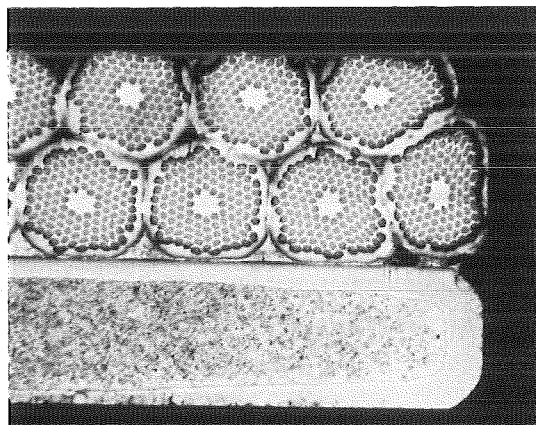


Fig. 8: Cross section of the composite conductor

A prototype sample of about 70 m of composite conductor had already been manufactured by industry. This length was used to wind a 12 layer test coil. A test in the 11.5 T background field of HOMER confirmed the expected properties of the conductor with respect to the current carrying capacity and the mechanical load carrying ability. It was demonstrated that an industrial manufacturing of the composite without introducing any damage into the conductor is feasible. After improving the spatial temperature homogeneity of the oven the heat treatment of the 1000 m flat cable was carried out. At present the arrangement suited for the careful rewinding of the brittle conductor onto a storage spool is being installed.

Optimization of alloyed Nb₃Sn multifilamentary wires

In view of the development of Nb₃Sn fusion conductors, the question arises whether the filament diameter has

an influence on the critical current density of the superconducting wires. This problem has been studied at the Institute of Technical Physics on a Ta alloyed Nb_3Sn multifilamentary wire prepared by the bronze process.

The wire of originally 0.86 mm diameter was drawn to the diameters 0.62, 0.44, 0.29 and 0.24, respectively and subsequently reacted at 700 °C during times reaching 200 hours. The results are represented in Fig. 9, where not only the various wire diameters but also the corresponding filament sizes and spacings are indicated.

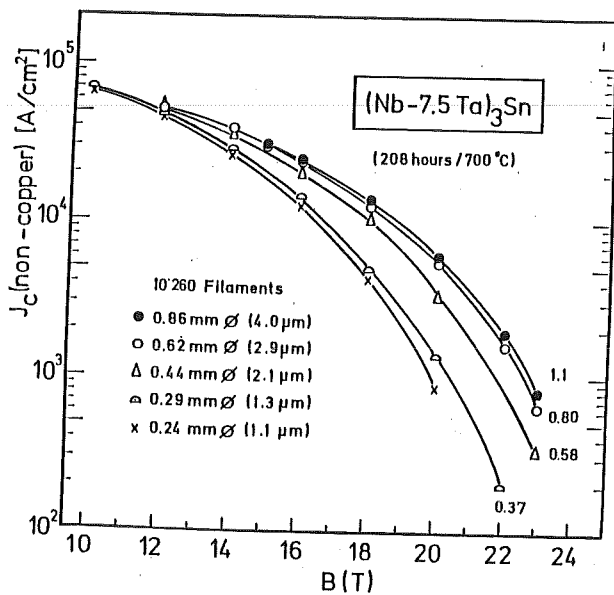


Fig. 9: J_c vs. B (non-copper) for Ta alloyed Nb_3Sn wires with diameters ranging between 0.86 mm and 0.24 mm. The corresponding filament sizes and spacings are also indicated.

The most surprising result is the cross-over of the J_c curves at ~ 12 T. Below 12 T, J_c is highest for the thinner wires (0.29 and 0.24 mm diameter), while at higher fields, the highest J_c values correspond to the thicker wires. The difference in J_c between thick and thin wires increases considerably with magnetic field and reaches an order of magnitude at 21 T. This

observation agrees with the fact that the upper critical magnetic field, B_{c2}^* , decreases gradually from 24.6 T for 0.86 mm diameter wires to 21 T for the thinnest wires.

In order to explain these results, we have proposed a correlation between B_{c2}^* and the state of compression of the Nb_3Sn filaments. Our model is based on the fact that the bronze matrix undergoes a considerable amount of plastic flow during the cooldown from 1000 to 4.2 K. This plastic flow is finally responsible for the discrepancy between observed and measured values of the compressive strain, ϵ_m . For bronze processed wires, the measured values for ϵ_m is close to 0.3 %, while the calculated value assuming elastic deformation only reaches 0.9 %. ϵ_m values of 0.7 % have so far only been measured on wires with ultrafine filaments, where the filament spacings are in the submicron range. The shift of ϵ_m to higher values can be explained by an increase of the elastic limit of the bronze matrix with decreased filament spacing (in the present case, the spacings diminish from 1.1 to 0.32 μm).

From the present results, the following important conclusions can be deduced:

1. High magnetic fields:

In order to optimize J_c at 20 T for Ta alloyed Nb_3Sn multifilamentary wires, the present work shows that two conditions have to be fulfilled, a) filament diameter/spacing larger than 6 - 8 μm /1 - 2 μm , and b) the reaction time (presumably at 700 °C) should be optimized for each filament diameter/spacing combination, but should exceed 200 hours, the diffusion process being slower than for binary Nb_3Sn . Observing these two conditions J_c values (non-copper) of $\geq 1 \times 10^4$ A/cm² at 20 T should be reached in Ta alloyed Nb_3Sn multifilamentary wires.

2. Intermediate magnetic fields ($B \leq 12$ T):

In this field region, precompression effects are small compared to compositional effects. The more favourable Sn composition gradient in fine filament is thus the dominant factor. For Nb_3Sn conductors for fields $B \leq 12$ T, the filament size should thus be of the order of 1 μm and the filament spacing in

the submicron range. This result is of importance when optimizing the superconducting wires for NET coils.

Staff:

W. Barth

M. Beckenbach

R. Berggötz

N. Brünner

P. Duelli

V. Fath

R. Flükiger

S. Förster

F. Gauland

S. Gauss

W. Goldacker

E. Gorenflo

A. Kling

P. Komarek

W. Lehmann

B. Lott

G. Nöther

H. Orschulko

J. Pytlík

A. Nyilas

H. Raber

T. Schneider

E. Seibt

W. Specking

S. Stumpf

D. Tabarsi

P. Turowski

M 4 Superconducting Poloidal Field Coils

Superconducting cable

A squared cable design has been selected for further industrial development. The cable can be seen in Fig. 10. It consists of an inner stainless steel tube with 13 subcables cabled around. Each subcable consists out of 6 wires around a CuNi core. The subcables are insulated in order to decrease the AC-losses.

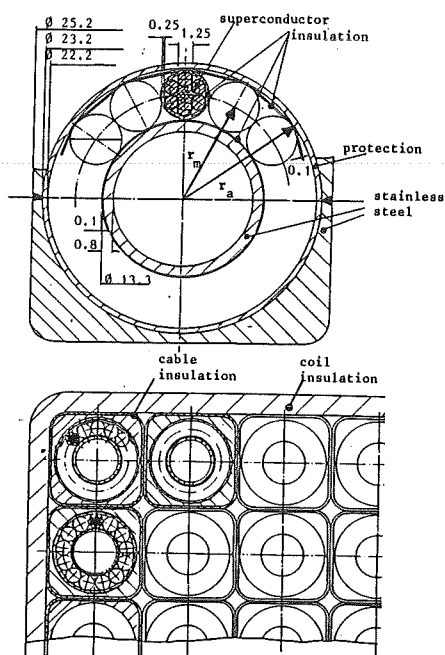


Fig. 10: Cable design and winding package for the model coil

A stainless steel casing with inner circular and outer quadratic shape was selected as vacuum tight enclosures of the cable. The selection was made after an industrial exploration of the possibility to fabricate the wanted U-shaped profiles. A call for tender for the development phase has been placed to different European firms.

Two phase flow experiment

The 200 m long test selection and the liquid He storage vessels have been mounted on the support structure (Fig. 11). The instrumentation with

temperature and pressure sensors is going on. The necessary changes in the cryogenic supply system of the TOSKA facility have been done. The vacuum vessel is now prepared for insertion of the test section.

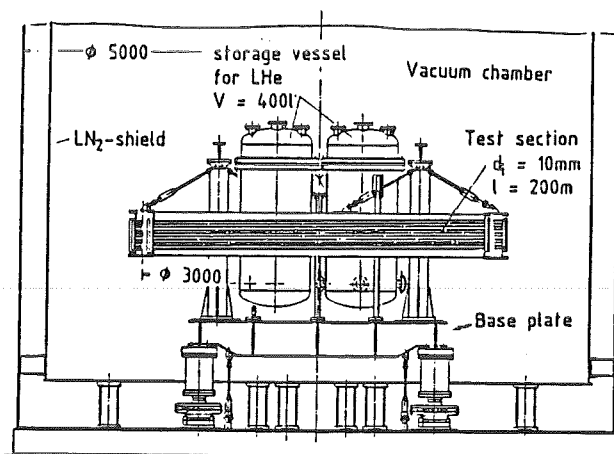


Fig. 11: Two phase flow test section mounted on the support structure inside the cryostat.

AC-loss measurements on the subcables

Further measurements on subcable samples have been carried out. Measurements of the contact resistance have been performed for different degrees of subcable compaction including complete soldering of the subcable. In all cases the ac-losses of a subcable surpass the losses of six individual wires only slightly, which proves a high contact resistance. This is well in agreement with theory. The measurements will be continued.

Current leads test

The current leads, which have been used in the TOSKA facility (for the LCT coil test) were tested in a bath cryostat with zero current.

The leads and the cryostat were equipped with 14 temperature sensors, levelprobes, mass flow sensors, pressure- and voltage taps before the test was run. The LCT-TOSKA data acquisition system (PDP11) was used.

The following data were taken at zero current:

- temperature versus length,
- mass flow of evaporating helium (loss),
- temperature difference between copper conductor and gaseous helium.

Zero current losses are 50 W per terminal. These losses are caused by the leads themselves not by superconducting buses as assumed before the test. Due to the high losses we could not operate the leads with current. The Helium supply with dewars would have given us time intervals too short for stable operation. Taking these test results into account, new leads shall be designed with some more length and a larger heat exchange surface. Current activities are collecting and evaluating basic data for the predesign of a new 30 kA current lead.

Predesign of the TORE-SUPRA-COIL

The predesign of the TORE SUPRA Coil has been started including components as winding package, pancake connection and current feed through.

In discussion with CEA/Cadarache questions of coil arrangement within TORE SUPRA cryostat were discussed and specifications for the mounting space were agreed upon.

Task sharing was rediscussed. KfK will deliver the coil and the cryogenic enclosure around the coil whereas CEA will provide the cryogenic supply and will contribute to manufacture of supports and current leads.

Staff:

H. Bayer
F. Beckenbach
F. Becker
S. Förster
G. Friesinger
U. Jeske
H. Katheder
P. Komarek
W. Lehmann
G. Nöther
A. Nyilas
H. Raber
L. Schappals
G. Schenk
C. Schmidt
K. Schweickert
L. Siewerdt
E. Specht
M. Süßer
A. Ulbricht
R. Wagner
D. Weigert
F. Wüchner

MAT 1 Post Irradiation Testing of Stainless-Steel

It is assumed that due to thermal fatigue the material of the first wall is subjected only to compressive plastic strains. The question now arises to what extent the number of cycles to fracture, N_f , depends upon the different loading conditions shown in the fig.12.

- a.) Compressive strain experiments (I)
- b.) Damage caused by tensile strains (II)
- c.) Deformation due to compressive strains followed by tensile strains (III)

In addition they are symmetrical in regard of the strain-axis. This behaviour was found at 450, 650 and 850°C. As a result of creep damage the number of cycles to fracture is decreased with increasing temperature. Concerning the three different loading types the N_f -values show - for a given temperature- almost no difference. Further tests at 20°C have still to be performed.

Since the fabrication of the specimens of AISI 316 and 1.4914 has not yet been finished, the LCF-tests were conducted on SS type 1.4948, heat 402.

Staff:

- W. Baumgärtner
- M. Bocek
- C. Petersen
- D. Rodrian
- W. Scheibe
- R. Schmitt
- H. Schneider
- W. Schweiger
- R. Tinivella

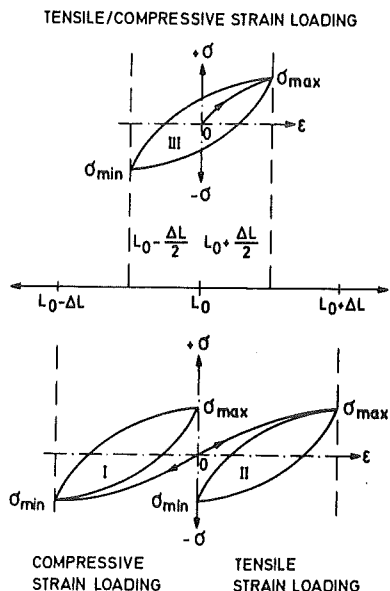


Fig.12: Different loading conditions of SS

One may expect that under comparable conditions the loading type with the most severe effects is that with tensile strains (II) whereas less damage expected to be produced under compressive strain (I). Low cycle fatigue test, however, reveal that the N_f -values for all three loading conditions are nearly the same. The reason for this could be that in the three cases considered the stress-strain-curves have a tensile stress-phase.

MAT 6/MAT 13 Ceramics for First Wall Protection,
Insulators and Windows

An irradiation test CERAM on various sets of ceramic samples in a TRIO capsule of the HFR-Petten was scheduled for May 1986. Half of the capsule space has been reserved for the partners of KfK (CEA and SIN). Two high temperature legs of the TRIO capsule (~1200°C) will be loaded with first wall materials, one low temperature leg (~400°C) with insulator materials. The maximum fast neutron fluence wanted is $1 \times 10^{22} \text{ n/cm}^2$ ($E > 0,1 \text{ MeV}$).

The assembling map for the samples is nearly completed, availability being expected in November 1985. The KfK samples will consist of three different types of SiC (MAT 6), of Al_2O_3 (commercial, highly pure, and single crystal), and of AlN (MAT13). Different sample shapes are intended for measuring 1) breeding strength, 2) Young's modulus, compressive strength and thermal shock resistance, 3) thermal expansion, 4) thermal conductivity, 5) electrical resistance and dielectric loss.

Up to now, the samples of two types of SiC, of single crystal Al_2O_3 , and of AlN are available. The examination of bending strength and thermal conductivity has been started (see also the preceding semiannual report). For HPSiC an appropriate level of preload testing was determined and applied to narrow the strength distribution of the irradiation samples.

Methods of measuring electrical properties are being introduced.

The thermal diffusivity of AlN was measured with a laser flash equipment.

The preliminary data were converted to thermal conductivity using:

$$c_p = 0,1 + 3,1 \cdot 10^{-3} T - 3,2 \cdot 10^{-6} T^2 + 1,1 \cdot 10^{-9} T^3$$

(mean value from /1,2/)

$$\rho = 3,3 (1 - 9,7 \cdot 10^{-4} T + 2,6 \cdot 10^{-6} T^2 + 2,0 \cdot 10^{-9} T^3)^{-3}$$

c_p specific heat at constant pressure, ρ density

$$[T] = \text{K}, [\rho] = \text{g/cm}^3, [c_p] = \text{J/g K}, 293 < T < 1640 \text{ K.}$$

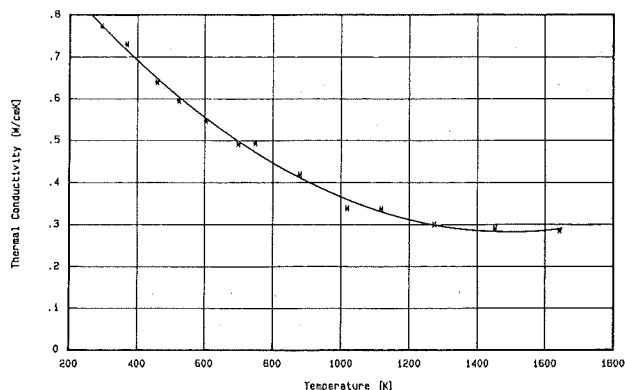


Fig. 13: Thermal conductivity of AlN (preliminary)

The equation for the temperature function of ρ is based on measurements of the relative linear thermal expansion of AlN by / 3 /. The conductivity data are shown in Fig. 13. They follow a simple $1/(a+bT)$ temperature dependence up to 1200. The material has nearly 100% density, its main impurities are 5-7% Al_2O_3 as second phase (see Fig. 14), metallic Fe, and probably carbon.

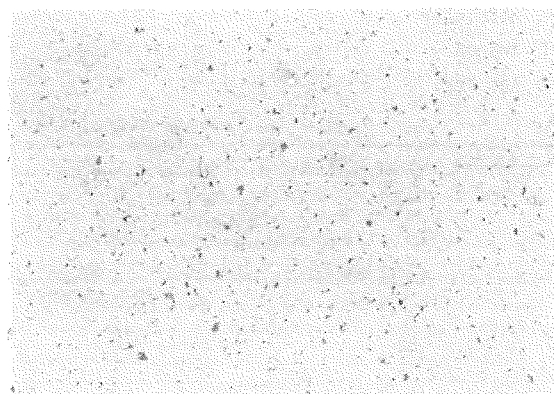


Fig. 14: Microstructure of AlN (as received), dark grey - Al_2O_3 , white-metallic impurities, 500x.

The samples are of black colour and have no significant optical transparency in the visible and infrared region (especially not at $1.06 \mu\text{m}$). From Fig. 14 would follow a much higher thermal conductivity for AlN (0.38 W/cmK) as was expected from 0.2 W/cmK in / 4 / at 1000 K. But it is not yet clear, whether this is caused by the impurities mentioned above. For comparison: (Al_2O_3 , 1000 K) = 0,080 W/cmK.

/1/ A.D. Mah, E.G. King, W.W. Weller, A.U. Christensen; US Bureau of Mines Report 5716 (1961)

/2/ R. Mezaki, E.W. Tilleux, F.T. Jambois, J.L. Margrave; III ASME Symposium on Thermal Physical Properties, Purdue 1961

/3/ U.M. Taylor, C. Linie, J. Electromechanical Soc. 107 (1960) 308

/4/ M. Billy, J. Mexmain, Sprechsaal 118 (1985) 245

Staff:

Ch. Adelhelm

W. Dienst

G. Gausmann

G. Grathwohl

R. Heidinger

H. Iwanek

V. Karcher

F. Porz

B. Schulz

S + E 1 Radioactive Effluents: Behaviour of
Gaseous Tritium in the Air, Plant, Soil System

The participation in the French Tritium Release Experiment has been prepared, in particular a sampling system for collecting HT and HTO in the environmental air has been completed. Inactive tests to find out convenient methods for separation of different plant components (protein, nucleic acids, polysaccharides and fats) are taking place.

Perspectives for the next reporting period:

- Participation in the French Tritium Release Experiment.
- Purchase of an oxidizer for low level measurements of tritium in large amounts of plant material.
- Purchase of a preparative ultracentrifuge for separation of nucleic acids, proteins and cell compartments by the method of density gradient centrifugation.
- Gaschromatographic studies on permeation of H₂ into different types of soils and humus layers under various climatic conditions are planned.
- The climatic chamber will be put into operation, inactive and later active tests will be carrying on.

Staff:

S. Diabate

D. Honig

L. König

H. Schüttelkopf

S+E 2 Accident Analysis

The actual activities concentrate on the availability and reliability analysis of substems (1) and on analysis of buckling phenomena (2).

1. Availability and Reliability Analysis of Subsystems

The special analysis of the protection system of a neutral beam injector has been terminated. The main results were explained in the preceding semi-annual report. The work performed and the detailed results are documented also in an internal report.

As a new topic the analysis of safetyrelated components of superconducting magnets has been chosen. The investigation starts with the analysis of the TESPE facility already in operation at KfK. The work will be performed in close collaboration between the Institute for Reactor Development and the Institute for Technical Physics to take advantage to the accumulated operational experience appropriately. Experience gained within this exercise will be applied for subsequent investigations of the NET-related subsystems.

2. Analysis of Buckling Phenomena

In continuing the development of a numerical computational method for the buckling analysis, our linear approximation method has been generalized.

The critical bifurcation load now can be calculated by assuming any initial imperfection. The comparison of the numerical results with closed form solution of elastic founded columns and hydrostatic loaded cylinders has proven to be good.

The linear approximation used up to now give a fast evaluation of the bifurcation load of an ideal configuration.

The modification of the critical values due to an imperfect geometry /21282/ is showing the right tendency but underestimates the sensitivity of the real structure.

Better results can be obtained using a nonlinear approximation. For this higher approximation a first concept has been realized. This nonlinear method is based on the linear approximation developed so far. Again linear FEM-calculations are used. The nonlinearity of the problem is taken into account by the disturbed initial geometry. The computational effort of this higher approximation method is roughly increased linearly with the order of nonlinearity, e.g. for a quadratic approximation one needs twice the effort of a linear calculation. Fig. 15 shows a first comparison of the linear and quadratic results for a ring. The typical imperfection sensitivity for small imperfection to wall thickness ratios U_0/S is approximated very well by a quadratic approximation. In addition and for comparison the result of a calculation by the ADINA code is included in Fig. 15.

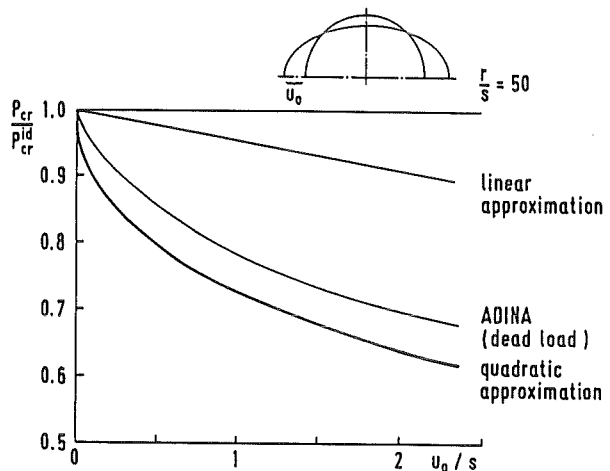


Fig. 15: The influence of initial imperfections on the buckling load of a ring
 (r = radius, s = wall thickness,
 U_0 = initial imperfection)

The method of nonlinear approximation has to be developed further on. It has to be investigated which order of approximation is sufficient for a given geometry.

Staff:

B. Dolensky
W. Kramer
R. Krieg
S. Raff
H. Schnauder

Publication:

21282

T 1 Fuel Clean-up System

As announced in previous semi-annual reports, a technical fuel clean-up test unit with a flow-rate smaller than NET-scale was defined and the basic design carried out. This work was concluded and documented.

The proposed unit, containing different clean-up process components, in line or in parallel, had the objective to develop the optimum process combination for the NET-fuel clean-up system.

As a result of discussions with CEA and the NET team, more fundamental work on specific clean-up process (getters, permeation membrans, catalysts) was felt necessary before carrying out an integral test of technical scale. This has led to a new definition of tasks for the 85/89 programme.

In addition to these studies of fundamental effects, the design of a clean-up unit of NET scale shall be further elaborated.

We therefore proposed to compile the design parameters for such a loop, based on the previous work, to design the installation beginning with flow sheet studies.

Staff:

J. Hanauer
E. Hölzchen
E. Hutter
G. Neffe
P. Schira
U. Tamm

T 5 Development of Tritium Decontamination Systems

The experimental facility employed for the investigation of the hydrogen permeation through nafion has been described in detail in a previous report. Briefly, argon carrier gas, in a 238 l loop, containing between 0,9 and 4,2 % vol. of a certain impurity, is passed through a bundle of 50 nafion tubes having a diameter of 0.1 and a length of 200 mm. Argon sweep gas from 70 l closed loop is passed at considerably lower pressure in counter current along the outside of the nafion tubes. The concentration decrease of the impurity in the large loop as well as the gas permeated into the small loop is followed gas-chromatographically over a period of several days. So far the following impurities, characteristic to the fusion fuel cycle, have been examined: H₂, CO, CO₂ and CH₄. In addition first results have been obtained with NH₃ and H₂O.

Figures 16 and 17 show typical results obtained with H₂, employing the above described procedure. It is seen that the amount of H₂ permeation is directly proportional to the time and directly dependent upon H₂ concentration in the carrier gas.

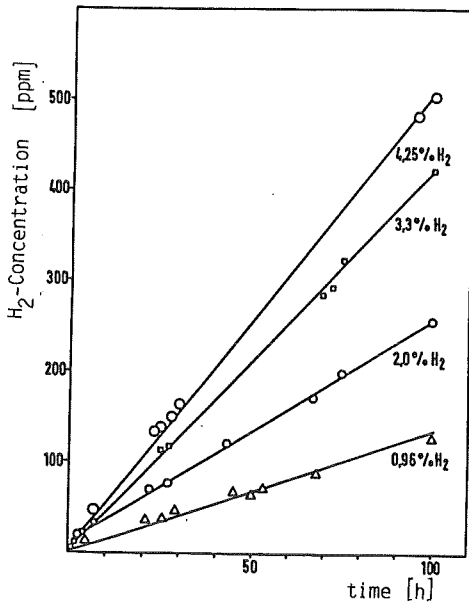


Fig. 16: Effect of temperature on the permeation of hydrogen through a bundle of nafion tubes PD-750-12P

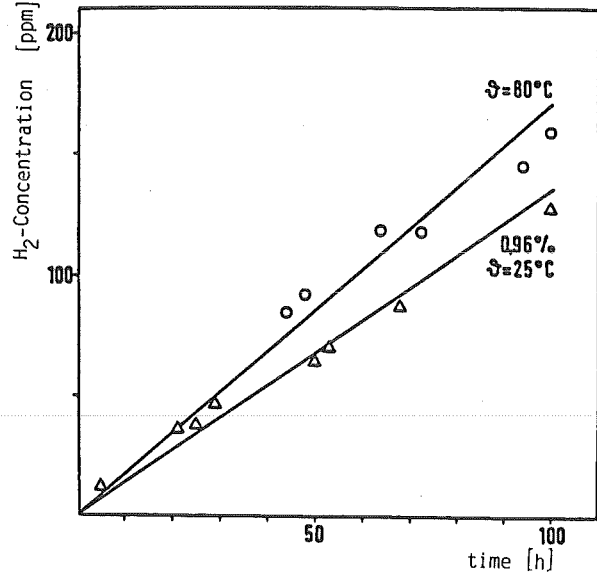


Fig. 17: H₂ permeation through a bundle of nafion tubes PD-750-12P

Similar results were obtained with CO₂. The permeation of CO and CH₄ was very low. Even after a period of one week the amount permeated into the sweep gas could not be detected gaschromatographically.

Still preliminary data suggested the following relative rate of permeation

H ₂ O	NH ₃	H ₂	CO ₂	CH ₄ , CO
------------------	-----------------	----------------	-----------------	----------------------

Experiments with another bundle of nafion tubes, having considerably more surface area, are in progress. The evaluation of these data will complement those obtained previously and permit an estimation of permeation coefficients.

The available information, together with tests presently under way on the resistance of nafion to its application in fusion technology.

Staff.

R.D. Penzhorn

M. Sirch

E. Willin

T 6 Industrial Development of Large Components
for the NET Vacuum System

1. Component Development

Following the invitation to bid the firms quoted to prepare the reliability studies for the turbomolecular pumps (50,000 l/s helium). The ad hoc group T 6, in conformity with a KfK suggestion, selected one of the three quotations and submitted it to the Fusion Technology Steering Committee for approval. The order to be placed in October 1985.

The technical specification for the all-metal valves, NW 1500 mm, was revised to adapt it to the alternative solution of the torus vacuum system with turbomolecular pumps. It appeared that the operating conditions for the valves are so different that two separate specifications are needed for the two variants of turbomolecular pumps and cryopumps. The number of closures is particularly crucial as regards the service life of the valves. The high number of 30,000 regeneration processes required for the cryopumps on account of the limited amount of tritium inventory calls for an accordingly high number of closures. On the other hand, for reasons inherent in operation not more than 100 closures must be anticipated with the version involving turbomolecular pumps. A preliminary inquiry including this new specification has been made.

Regarding the cryopumps, a specification has been elaborated for the feasibility study. The list of interested firms has been completed. Inquiries to industry will be sent by end of this year after discussion in the ad hoc group.

2. Component Testing

Within the framework of the feasibility study for the large component test facility the following work was performed:

The plant vacuum system has been designed for operation with and without tritium.

The gas feed system for simulation of the pulsed pressure originating from a tokamak divertor has been conceived and designed.

The anticipated shock loading of the components as expected by plasma disruptions, is simulated in a shock test bench. It is possible to generate in an alternative mode semi-sinoidal pulses, rectangular pulses and sawtooth pulses both in the vertical and horizontal directions.

In order to test the influence of solid particles on the operating behaviour of components a dust feed system can be installed into the vacuum vessel of the test arrangement. In this way, transport and deposition behaviour of various fusion reactor materials can be measured.

Three alternative installation concepts were studied for the component test area. Connection to the tritium laboratory was provided to have access to the tritium storage and recovery systems of this facility.

Staff:

J. Hanauer
W. Höhn
U. Kirchhof
H. Lukitsch
A. Mack
D. Perinič

Studies for NET/INTOR

12 NET study contracts were proceeding during the period of the progress report, some of them have been completed, others are continuing further on.

The "Initial CAD Investigations for NET" were completed, the final report was issued.

Based on NET2A data, a section of the torus has been modelled including magnets, blanket modules, shielding, divertor drawer. Various techniques for treating remote handling operations with CAD systems were investigated. An extension of the CAD system BRAVO! was developed which now allows the definition, analysis, and dimensioning of path for remote handling operations using traces of selected points of the moved components for visualization (Fig. 18).

Low level CAD data transfer has been investigated. A particular solution (a combination of the private network EARN and the public network DATEX-P) was selected and successfully tested. For high level data transfer of two- and three-dimensional wire-frame geometry the IGES standard format was selected. A wire-frame model of the JET boom produced with the CAD system BRAVO! was successfully processed by the IGES processors of MEDUSA and return to BRAVO!.

A preliminary analysis of the abstract information structures for the CAD area in the NET project has been made.

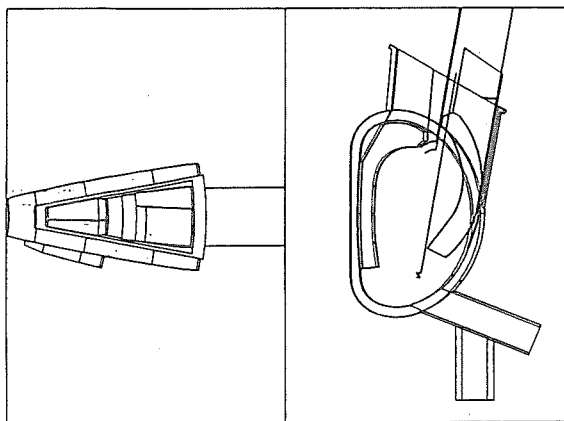


Fig. 18: Removal of the broader outboard blanket modules using BSIM: straight lines showing motion traces.

Also completed was the task "Compilation of Data and Properties of Lithium silicates".

Thermal conductivity, specific heat and thermal expansion are treated under thermophysical properties. Melting temperature, phase diagrams, phase change characteristics, enthalpy of formation and vapour pressures are treated under thermodynamic properties. Nothing could be found about the solubility of hydrogen or water in lithium silicate, the absorption of water or the formation of LIOH under water vapour.

Chemical interaction was confined to the compatibility with cladding material and with beryllium. Mechanical properties dealt with are elastic constants, especially Young's modulus, compressive strength and compressive creep behaviour. Since virtually nothing is known on irradiation effects in Li_2SiO_3 , this chapter gives only a brief assessment of the main topic, especially tritium diffusivity.

For the study concerning the "Evacuation Behaviour of NET-Design Alternatives", the final report was completed too.

One unique design feature of NET is given by the much greater number and variety of components installed inside the vacuum chamber with large and different kinds of surface areas exposed to the vacuum. In a first attempt, the pre-evacuation process was investigated for this new configuration. The results show, that with the anticipated pumping speed of $10 \times 50 \text{ m}^3/\text{s}$ of the turbomolecular pumps and an assumed realistic vacuum duct configuration, including the divertor channel, an acceptable pump-down characteristic can be achieved. However, because of the flow restrictions within the vacuum chamber by the different components installed (e.g. the blanket modules) remarkable pressure differences are created. Typical pressure-versus-time curves are given in Fig. 19.

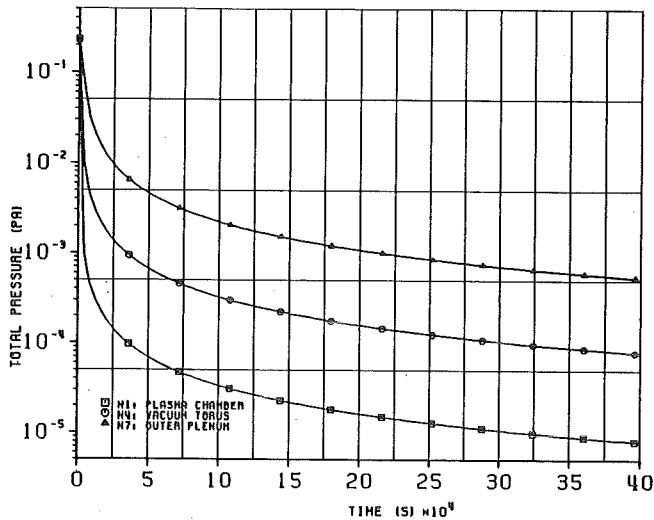


Fig. 19: Pressure During Evacuation

For the study on "Formulation of Initial Design Equations for Type 1.4914 Martensitic Steel", the final report is under preparation.

A comparison of the structural properties of the class of 9-12% Cr bearing steels has been elaborated. Within this class, type 1.4914 is a niobium-stabilized fully martensitic steel. The existing data on the physical metallurgy of Type 1.4914 have been compiled and the specification for a reference pretreatment and fabrication procedure has been defined. Thermophysical and elastic properties of type 1.4914 steel have been formulated as design equations. Available plastic properties like tensile-, creep-fatigue- and impact-properties have been compiled for the 9-12% Cr steels in comparison to Type 1.4914 steel. A literature search on the corrosion behaviour of the martensitic 9-12 % steels in liquid Li and Li-Pb and its influence on the creep-strength and fatigue-behaviour has been elaborated.

The Study "Pipe and vacuum duct connection" was completed too. It showed that, if possible, cutting / welding techniques should be preferred because non-destructive pipe connections using flanges, gaskets and clamping devices have many disadvantages. Thus the study contains a comprehensive description of the

state of the art of welding equipment and the recommended cutting and leak detection methods. Besides a survey of the existing remotely operated mechanical pipe connectors together with a general evaluation of their qualities is given and the most important sealing techniques are discussed. It is stated in the study that no existing connection system meets all requirements. Yet some systems and techniques are available which are proposed as a basis for further development work. The fields of large mechanical connectors for restricted access conditions and quality assurance for all types of connections need particular attention.

For the study "Vacuum Tight Connections and Closures on the Vacuum Vessel - Lip Welding and Cutting" the intermediate report was completed. Main subject is the investigation of the state of the art in lip welding and remotely operated cutting. It is shown that no existing welding and cutting technique meets all NET requirements. As a result of the discussion with the NET-Team, the requirements were slightly modified. In the draft for the final report the different methods are compared and the properties and maturity are described. As conclusion it is suggested to initiate a R&D programme to develop a modular welding / cutting system the general layout of which is based on results of the investigations and tests which have been carried out by KfK.

The work on "Design of the NET Equilibrium Poloidal Field Coils" was completed, and as far as the present study goals are concerned the draft of the final report was delivered. Based on the poloidal current which the NET team has calculated for machines of different types and sizes, this study presents a design of a superconductor able to carry 40 kA at 6 T, and a layout of coil windings for three different poloidal field coil systems. The conductor resembles the LCT type of EURATOM/KfK, but is made suitable for the application in coils with moderate pulse rates. For the case of higher rates, an alternative conductor as developed for the task M 4 with lower AC losses was sketched. Concerning the windings there are given data about the start-up voltages, the cooling requirements and the loadings.

Fig. 20 shows the principles of the reference conductor used in the design.

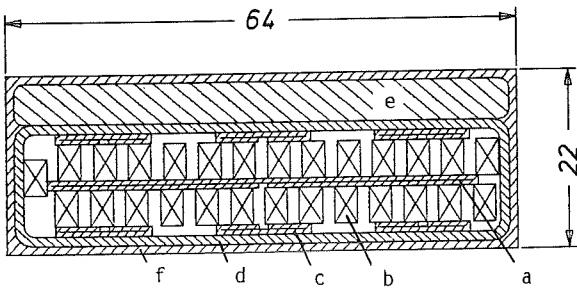


Fig. 20: Conductor for NET equilibrium poloidal field coils.

- a - core, $54 \times 1.2 \text{ mm}^2$
- b - s.c. strands (Cu/CuNi-matrix)
 $27 \times 2.8 \times 4.5 \text{ mm}^2$
- c - steel strips, $6 \times 12 \times 1.2 \text{ mm}^2$
- d - steel case, $62 \times 15 \text{ mm}^2$ outside,
1.2 mm thick
- e - steel reinforcement, $62 \times 5 \text{ mm}^2$
- f - insulation, 1 mm thick

In comparison to the LCT conductor, there are mainly three changes. Firstly the current carrying capability is doubled, secondly the superconducting strands contain CuNi, reducing the AC losses inside of the strands, thirdly the distance between neighbouring strands relative to the strand was enlarged.

At the Roebel transition, contacts between the strands, which have proven to cause AC losses in the LCT conductor, will thus be avoided during manufacturing. For the present NET conditions, the total AC losses of the described conductor look tolerable. Concerning the heat pulses due to fast field changes, the rise of the temperature in the conductor is always so low, that no extraordinary cooling modes are necessary in order to ensure stability. Mechanically, the conductor is expected to be as stable as the LCT conductor. During the current initiation, the maximum inductive voltage in a single coil is about 23 kV. This is the same value as for the poloidal field coil now under design at KfK (task M 4). Testing of this coil should provide the necessary experience.

The study "Stress and Lifetime Calculations" has been continued. In the actual NET-design of a helium cooled first wall a plane wall is proposed containing rectangular cooling channels. For this structure analytically given formulas were derived to describe the stationary temperatures due to surface heat flux as well as volumetric heating by neutron irradiation. Fig. 21 shows the normalized stationary temperature distribution in a first wall segment caused by pure surface heat flux. The influence of geometric data on maximum surface temperatures is described by approximative equations.

For a NET first wall design with inner coolant tubes transient temperatures (considering also the influence of several possible dwell-times on temperature differences during one cycle) and thermal stresses are calculated by finite element methods.

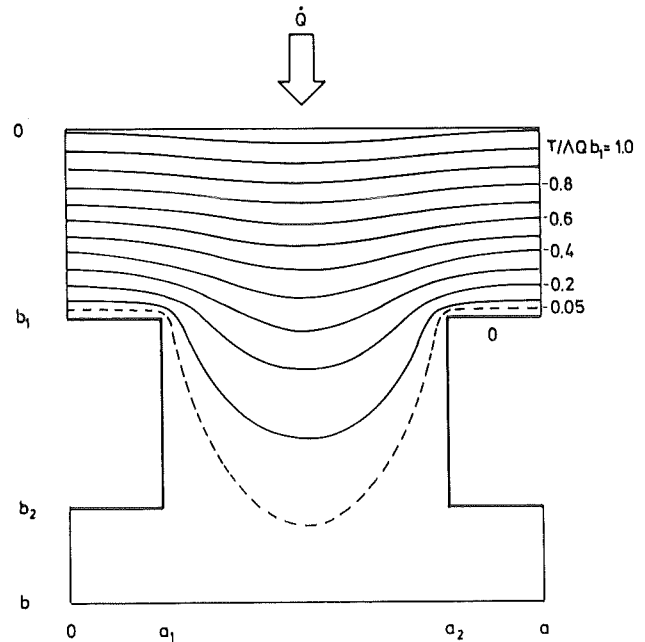


Fig. 21: Stationary temperature distribution in a first wall segment

The draft final report of the study "Design of a quasi-optical ECRH transmission system for NET/INTOR" was submitted. A conceptual design of a quasi-optical ECRH transmission system for 140 GHz and 10 MW is described. Eight beam waveguides of 40 cm diameter are proposed to launch 10 MW over 100 m. Each beam waveguide is fed by a 12 cm diameter Gaussian beam formed by combining the output powers of four 350 kW, 140 GHz gyrotrons. The beam waveguide consists of five 40 cm diameter dielectric lenses. The lens spacing is 20 m. Double-disk ceramic windows of also 40 cm diameter are necessary as a tritium barrier at the plasma end. Problems of windows, lenses and beam waveguide launcher are discussed. Open questions are listed.

A "Scoping study on structural low electrical conductivity and insulation materials for NET magnet systems" was started. The study concentrates on glass-, carbon- and kevlar fibre composites with epoxy, polyimide and thermoplastic matrices. Data on resistance against irradiation, gas permeation and fibre-matrix interfacial bond properties are already collected. Mechanical, thermal and electrical properties are under compilation now.

Based on the results of the preceding NET-TF-coil conductor study, a "TF coil design effort" has been started. The work is performed in close collaboration with SIN, ECN and ENEA, to whom identical contracts have been awarded. In common meetings several tasks have been treated so far. Subject of the study are procedures for the calculation of AC losses, the mechanical aspects of the coil design, the choice of the conductor current, the coil protection philosophy and the cryogenic system.

Staff:

F. Arendt
G. Böhme
G. Class
E. Diegele
W. Dienst
K. Ehrlich
J. Erb
T. Fett
R. Flükiger
G. Hartwig
B. Haferkamp
U. Jeske
W. Katz
P. Komarek
M. Kuntze
K. Leinemann
J. Lühning
A. Ludwig
U. Marek
R.A. Müller
D. Munz
W. Olbrich
E.G. Schlechtendahl
K. Schramm
B. Schulz
M. Selig
A. Skokan
H. Zimmermann

Publication:

21160

Development of ECRH Power Sources at 150 GHz

1. Gyrotron Components

The microwave performance of the double disk output window and of the TE_{031} -resonator was measured. Operation frequencies, which critically depend on the mechanical tolerances of these components were found to approach the design frequency volumes within a tolerance of 0.5 GHz. Assembly of all parts of the gyrotron tube is now under preparation. Further development was started to make the output window tunable for operation at various rf-modes.

2. Gyrotron Theory

The parameter studies for the beam-rf interaction have been extended to study mode competition, in particular for the TE_{032} , TE_{231} and TE_{521} modes. Includes in the description of mode competition was the start dynamic response at start-up.

In an additional analysis, whispering gallery modes were analysed. For this type of modes, efficiencies between 30 % and 40 % were calculated.

3. Gyrotron Test Facility

Construction work in the experimental area was finished. The Faraday cage, which houses the high voltage components, and the control room were installed. The microsecond pulse power supply and the capacitor bank were set-up.

Manufacturing of the long pulse/cw modulator and the superconducting magnet system are in progress. Components for liquid Helium supply and gas recovery from the cryostat were ordered.

4. Microwave Diagnostics

A mode analyser for far-field measurements of arbitrary mode mixtures at the openend of an oversized

waveguide is under construction.

Fast spectrum analysis was provided by a preliminary set-up using a dispersive SAW-line. Further development is required for use in the mode competition experiments.

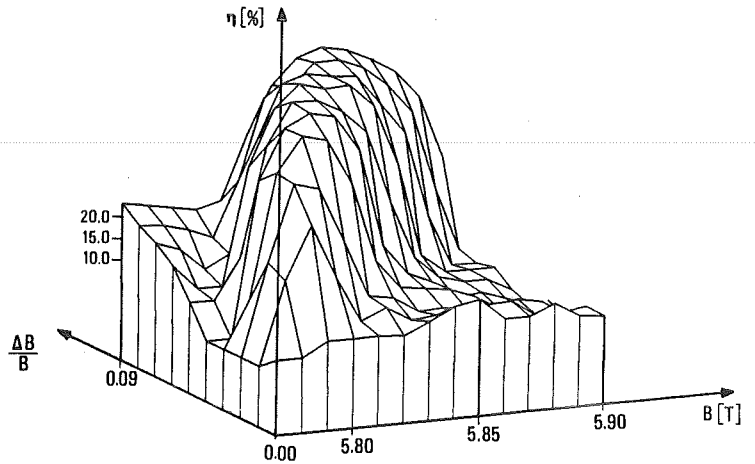


Fig. 22 : Efficiency as a function of magnetic field and magnetic field gradient for a cylindrical test resonator (length 15mm) in the TE_{031} -mode at 200 kW output power. The maximum efficiency at 55 % is reached at a magnetic field strength of 5.85 T with a field gradient of 8 %.

Staff:

E. Borie
H. Budig
G. Dammertz
S. Fenyi
F. Graf
P. Grundel
R. Hietschold
G. Hochschild
A. Hornung
K. Jentzsch
M. Kuntze
W. Maurer
N. Münch
H. Oppermann
B. Piosczyk
G. Redemann
H. Stickel
R. Vincon

External Contributors:

K. Behm and team (Valvo, Hamburg)
E. Jensen et al. (TU, Hamburg-Harburg)
M. Kitlinski et al. (IHE, Univ. Karlsruhe)
M. Thumm et al. (IPF; Univ. Stuttgart)
E. Dumbrajs (Abas, Leopoldshafen)

- V19929 VOLLATH, D.; WEDEMEYER, H.; GUENTHER, E.
Improved methods for fabrication of LiAlO_2
and Li_2SiO_3 pellets and spheres as breeder
material for fusion reactors.
13th Symp. on Fusion Technology, Varese, I,
September 24-28, 1984
- 21158 IMF;
WEDEMEYER, H.; VOLLATH, D.; GUENTHER, E.
Journal of Nuclear Materials (in press)
- 21160 ITP;
FLUEKIGER, R.; ARENDT, F.; HOFMANN, A.;
JESKE, U.; JUENGST, K.P.; KOMAREK, P.;
KRAUTH, H.; LEHMANN, W.; LUEHNING, J.; MANES,
B.; MAURER, W.; NYILAS, A.; SPECKING, W.;
TUROWSKI, P.; ZEHLEIN, H.
An A15 conductor design and its implications
for the NET-II TF coils. Final study report.
KfK-3937
- 21282 PKF;
FINKEN, D. [HRSG.]
Fusion technology programme. Semi-annual
report October 1984 - March 1985.
KfK-3922 (Mai 85)
EUR-9608e (Mai 85)

Appendix I: Participation of KfK Departments in the Fusion Technology Programme

Task Code No.	Title	KfK Departments	Partners
B 1	Blanket Design Studies	Institute for Neutron Physics and Reactor Engineering (INR) Institute for Reactor Components (IRB)	CEA; ENEA; JRC Ispra; KFA; UKAEA; Industry
B 2	Development of Computational Tools for Neutronics	Institute for Neutron Physics and Reactor Engineering (INR)	CEA; ENEA; FOM/ECN
B 6	Corrosion of Structural Materials in Flowing $\text{Li}_{17}\text{Pb}_{83}$	Institute for Materials and Solid State Research (IMF)	CEA; SCK/Mol
B 9	Tritium Extraction Based on the Use of Solid Getters	Central Engineering Department (IT)	JRC Ispra; SCK/Mol
B 11-B 16	Ceramic Breeder Materials	Institute for Materials and Solid State Research (IMF) Institute for Neutron Physics and Reactor Engineering (INR) Institute for Radiochemistry (IRCh)	CEA; ENEA; FOM/ECN; KFA SCK/Mol; UKAEA
M 1	Large Coil Project	Institute for Technical Physics (ITP) Institute for Data Processing in Technology (IDT)	IEA agreement: USA, Japan, Switzerland, EC; Industry
M 3	Development of High Field Composite Superconductors	Institute for Technical Physics (ITP)	CEA; ENEA; FOM/ECN; SIN/EIR
M 4	Poloidal Field Coils	Institute for Technical Physics (ITP)	CEA
MAT 1	Post Irradiation Testing of SS	Institute for Materials and Solid State Research (IMF)	CEA; FOM/ECN; SCK/Mol; Studsvik
MAT 6/ MAT 13	Ceramics for First Wall Protection, Insulators and Windows	Institute for Materials and Solid State Research (IMF)	CEA; SCK/Mol; UKAEA
S+E 1	Radioactive Effluents: Behaviour of Gaseous Tritium in the Air, Plant, Soil System	Central Safety and Security Department (HS)	CEA; Studsvik
S+E 2	Accident Analysis	Institute for Reactor Development (IRE)	CEA; FOM/ECN; JRC Ispra; Risø
T 1	Fuel Clean-up System	Institute for Technical Physics (ITP) Central Engineering Department (IT)	CEA; KFA
T 5	Decontamination System	Institute for Radiochemistry (IRCh)	CEA
T 6	Industrial Development of Large Components	Central Engineering Department (IT)	CEA
Gyrotron Studies		Institute for Nuclear Physics (IK) Institute for Data Processing in Technology (IDT)	Industry; Universities

Appendix II: Table of NET Contracts

Theme	Contract No.	Working Period
Stress and Lifetime Calculations for First Wall and Blanket Structural Components in NET	155/84-5/FU-D/NET	6/84 - 5/86
Initial Investigation of CAD Techniques for NET	164/84-7/FU-D/NET	6/84-5/85
Electron Cyclotron Wave Launcher for NET/INTOR	162/84-6/FU-D/NET	6/84 - 6/85
Formulation of Initial Design Equations for Type 1.4914 Martensitic Steel	171/84-9/FU-D/NET	10/84 - 3/85
TF-Coil Design Contract	183/84-12/FU-D/NET	12/84 - 12/86
Vacuum Tight Connections and Closures on the Vacuum Vessel-Lip Welding and Cutting	185/84-12/FU-D/NET	12/84 - 7/85
NET/INTOR Maintenance and Remote Handling Techniques-Support for Specific Tasks	193/85-2/Fu-D/NET	2/58-12/85
Scoping Study on Structural Low Electrical Conductivity and Insulation Materials for NET Magnetic Systems	194/85-3/Fu-D/NET	3/85- 9/85

Appendix III: KfK Departments and Project Management Group

Kernforschungszentrum Karlsruhe GmbH
 Postfach 3640
 D-7500 Karlsruhe 1
 Federal Republic of Germany
 Telephone (07247) 82-1
 Telex 7 826 484
 Telefax/Telecopies (0)07247/82 5503

KfK Department	KfK Institut/Abteilung	Director	Tel.
Central Safety and Security Department	Hauptabteilung Sicherheit (HS)	Prof. Dr. H. Kiefer	2660
Institute for Data Processing in Technology	Institut für Datenverarbeitung in der Technik (IDT)	Prof. Dr. H. Trauboth	5700
Institute for Nuclear Physics	Institut für Kernphysik II (IK)	Prof. Dr. A. Citron	3502
Institute for Materials and Solid State Research	Institut für Material- und Festkörperforschung (IMF)	I. Prof. Dr. F. Thümmler	2918
		II. Dr. K. Anderko	2902
		III. Prof. Dr. K. Kummerer	2518
Institute for Neutron Physics and Reactor Engineering	Institut für Neutronenphysik und Reaktortechnik (INR)	Prof. Dr. G. Keßler	2440
Institute for Reactor Components	Institut für Reaktorbauelemente (IRB)	Prof. Dr. U. Müller	3450
Institute for Radiochemistry	Institut für Radiochemie (IRCh)	Prof. Dr. H.J. Ache	3200
Institute for Reactor Development	Institut für Reaktorentwicklung (IRE)	Prof. Dr. D. Smidt	2550
Central Engineering Department	Hauptabteilung Ingenieurtechnik (IT)	DI W.P. Schmidt	3001
Institute for Technical Physics	Institut für Technische Physik (ITP)	z.Zt. Prof. Dr. P. Komarek	2653
Nuclear Fusion Project - Project Management	Projekt Kernfusion - Projektleitung (PKF-PL)	Dr. J.E. Vetter	5460
Secretary	I. Sickinger		5461
Administrator	Dr. D. Finken		5462
Blanket, Facilities	DI H. Sebening		5464
Superconducting Magnets,			
ECR-Heating	N.N. (Dr. J.E. Vetter)		5460
Tritium, Materials	Dr. H.D. Röhrig		5463
System Studies	Prof. Dr. P. Komarek		2653